J. Membrane Biol. 28, 373–399 (1976)

Electrophysiological Properties of Tissue Cultured Heart Cells Grown in a Linear Array

Frederick Sachs*

Laboratory of Biophysics, IR, National Institute of Neurological and Communicative Disorders and Stroke, National Institutes of Health, U.S. Public Health Service, Department of Health, Education and Welfare, Bethesda, Maryland, and Department of Physiology, State University of New York, Upstate Medical Center, Syracuse, New York

Received 23 June 1975; revised 6 February 1976

Summary. Embryonic chick heart cells were grown in tissue culture on an oriented substrate (channels cut in an agar coated slide), so that they formed narrow (5–100 μ) strands of arbitrary length. The electrical properties of these strands were examined using intracellular microelectrodes. ac and dc cable studies were performed to determine the passive cable parameters. Quantitative histology, using light and electronmicroscopy, permitted calculation of intrinsic capacitances and resistivities.

Electrical coupling between polarizing and recording electrodes was ubiquitous, falling off exponentially with distance. It was concluded that individual cells were electrically connected, since coupling was observed at distances greater than 3 mm, and the maximum cell length was estimated to be less that 300 μ. The strands were usually spontaneously active, with phase 4 depolarization (pacemaker potential) occurring almost simultaneously in all cells of a strand.

The passive electrical properties determined during phase 4 were: core resistivity (cytoplasm plus cell-to-cell resistance), 245 ohm/cm; membrane capacitance, 1.46 μF/cm^2. The membrane resistance increased from 16 to 136 kohm/cm^2 during phase 4. The space and time constants showed commensurate changes, from 0.95 to 3.2 mm, and from 29 to 269 msec, respectively. The input resistance also increased, from 1.1 to 3.8 Mohm.

The electrophysiology of the heart has been difficult to study due, not only to the complex currents that each cell may produce, but the presence of a variety of cell types and the elaborate coupling between them. In order to simplify the latter problems, a number of researchers have resorted to examining cells in tissue culture (DeHann & Fozzard, 1975; Lieberman, Sawanobori, Kootsey & Johnson, 1975; Sperelakis, 1967; Hyde, Blondel, Matter, Cheneval, Filloux & Girardier, 1969; Jongsma & van Rijn, 1972; and others).

* *Permanent address:* Department of Pharmacology and Therapeutics, State University of New York, School of Medicine, 122 Farber Hall, Buffalo, New York.

Observations on the electrical properties of tissue cultured cells agree qualitatively with the responses observed *in vivo* (Sperelakis, 1967; Lieberman, 1973). The present experiments show that the passive electrical properties of cultured chick heart strands are similar to those of other cardiac tissue. The cultured cells show anomalous rectification, an increase in slope resistance during the plateau, voltage sensitive repolarization, and time-dependent conductance decreases during phase 4 as observed in the Purkinje fiber (Weidmann, 1951, 1952, 1955), and other cardiac tissues (*cf.* Cranefield & Hoffman, 1958; Fozzard & Sleater, 1967; Giebisch & Weidmann, 1967; Rougier, Vassort & Stampfli, 1968; Johnson & Tille, 1960).

Most studies in tissue culture have used monolayer cultures. There are quantitative reports on electrotonus in sheet cultures (Hyde *et al.*, 1969; Jongsma & van Rijn, 1972). Hyde *et al.* (1969) had good histological data and some degree of control over the myoblast/fibroblast content of the cultures. In "pure" myoblast cultures they found values for the cytoplasmic and membrane resistivities (ρ_i and ρ_m, respectively) which are in good agreement with those found in this study. They found a linear current-voltage relationship. In mixed fibroblast-myoblast cultures they found lower membrane resistances and higher core resistivities. Jongsma and van Rijn extended Hyde *et al.*'s measurements by observing the electrotonus time response from which they derived a reasonable value for the membrane capacitance (1.3 $\mu F/cm^2$). However, as shown by Noble (1962), studies of electrotonus in such planar core conductors is a very insensitive way to establish membrane parameters.

The ideal preparation for the study of cell membrane properties would be a single isolated cell devoid of intercellular connections. Unfortunately, penetration of isolated cells with one, let alone two microelectrodes is extremely difficult. (DeHaan & Gottlieb, 1968; Lehmkuhl & Sperelakis, 1963). The next simplest preparation, and the simplest preparation that includes the effects of intercellular connections, is a "one dimensional" string of cells, analogous to the Purkinje fiber preparation. As shown in this paper, such "one dimensional" strands may be grown in tissue culture by proper preparation of the substrate (*see also* Lieberman *et al.*, 1975).

The cultured strand preparation described in the present paper has a number of advantages over conventional cardiac preparations for the study of electrical properties. For one, small diameter strands may be obtained without the necessity of dissection and consequent tissue damage. Secondly, cells may be spatially arranged as desired to best fit

the experimental requirements. Short strands are simple to prepare and may be useful for microelectrode voltage clamping.

A sucrose gap voltage clamping system might be made by growing the cells directly in a photoetched sucrose gap apparatus made to extremely fine dimensions since the strands are of small diameter and would not need to be handled. Furthermore, the strand might be allowed to spread out on either side of the control area to allow more area through which to drive the control currents. Thicker strands are easily removed from the dish and may be studied elsewhere.

In order to assess the suitability of the preparation for experiments on the active membrane properties, the passive properties of the preparation should be understood. To this end I have studied the small signal properties of the strands using sine wave and pulse measurements of the impedance (Sachs, 1969).

The results of this study are in remarkable agreement with those reported by Lieberman *et al.* (1975) on a similar preparation.

Theory

This section is included for reference and derivations are not included. The interested reader is referred to the more detailed treatments given by Hodgkin and Rushton (1964); Falk and Fatt (1964), and the publications of Eisenberg and his colleagues (*cf.* Valdiosera, Clausen & Eisenberg, 1974).

Some commonly used symbols are given below.

Symbols and Definitions

Variables.

x = distance from the stimulus in a one-dimensional cable, in cm.
t = time, in sec.
I = current in amp.
V = transmembrane potential measured from the resting value, in v.
ω = angular frequency, in radians/sec. $\omega = 2\pi f$, where f is frequency in Hz.

Intrinsic Constants.

ρ_i = specific resistivity of the core, in Ω-cm.
ρ_m = specific resistivity of the cell membrane, in Ω-cm^2.
C_m = specific capacitance of the cell membrane, in F/cm^2.

Extrinsic Constants.

R_m = membrane resistance times unit length, Ω-cm^2.
R_i = resistance per unit length of the core, in Ω-cm.
C = capacitance per unit length, in F/cm.
λ = DC space constant, in cm.
τ = membrane time constant, in sec.
R_0 = input resistance in Ω.
v = conduction velocity, in cm/sec.
T_{AP} = time constant of the foot of the action potential in sec.
SF = safety factor for propagation, dimensionless.

For a "one dimensional" core conductor, voltage produced by current injected at a point is described by the one dimensional cable equation:

$$\frac{d^2 V(\omega)}{dx^2} - R_i Y(\omega) = 0 \tag{1}$$

where Y is the membrane admittance.

The equation has been solved analytically for a variety of driving currents, membrane admittances and terminations. If we consider an infinitely long cable with a parallel RC admittance for the membrane, the voltage produced by a step of current, I_o, injected at $x=0$, and $t=o$, is given by Hodgkin and Rushton (1946):

$$V = R_i \lambda I_o/4 [e^{-X} \operatorname{erfc}(X T^{-1/2}/2 - T^{1/2}) - e^X \operatorname{erfc}(X T^{-1/2} + T^{1/2})] \tag{2}$$

where $X = x/\lambda$, $T = t/\tau$, and erfc is the complementary error function. In the steady state ($T=\infty$) the voltage decays exponentially with X providing a method for measuring the space constant. At $x=0$, the voltage changes proportional to $\operatorname{erf}(T^{1/2})$ where erf is the error function ($\operatorname{erf}(1) = 0.84$). Thus the time taken for the voltage to reach 84% of its steady state value is equal to τ. τ may also be estimated from a plot of the time to half amplitude as a function of distance, since to a good approximation, the half amplitude point travels with a velocity $2\lambda/\tau$ (Hodgkin & Rushton, 1946).

For sinusoidal currents the appropriate solution to Eq. (1) is given by Tasaki and Hagiwara (1957):

$$V = I_o R_i \lambda (1 + \omega^2 \tau^2)^{-1/4}/2 \cdot \cos(\omega \tau - n x/\lambda - \tan^{-1}(n/m)) \tag{3}$$

where

$$m = (1 + (1 + \omega^2 \tau^2)^{1/2}/2)^{1/2} \quad \text{and} \quad n = (-1 + (1 + \omega^2 \tau^2)^{1/2}/2)^{1/2}.$$

The equation may be better understood by looking at it in three parts. The first part, $R_i \lambda(1+\omega^2 \tau^2)^{-1/4}/2$, represents the absolute value of the input impedance as a function of frequency. The second terms, $e^{-mx/\lambda}$, represents the attenuation as a function of distance, where λ/m is generalized space constant which decreases with increasing frequency. And finally, the cosine term represents the time and phase relationship between the voltage at the origin and that at point x.

At high frequencies, the membrane capacitance carries most of the current through the membrane and the cable structure may be approximated as simply the core resistance and the membrane capacitance. The behavior of such a cable can be derived from Eq. (3) by considering the case where $\omega\tau \gg 1$. In that case, the amplitude of the voltage at distance x in response to a current $I_o \sin(\omega t)$ injected at $x=0$, is given by Tasaki and Hagiwara (1957) in the form:

$$\ln(V\omega^{1/2}) = \ln(k) - \omega^{1/2}/h \tag{4}$$

where

$$h = x^{-1}(2/(R_i C))^{1/2} \quad \text{and} \quad k = 1/2(R_i/C)^{1/2}.$$

Eq. 4 can be plotted as a linear graph, yielding values of h and k from the slopes and intercept, and hence, R_i and C.

Materials and Methods

Disaggregation and Plating Procedure

Whole hearts from 6 to 9 day old White Leghorn embryos were aseptically removed and placed in 5 ml of modified Hanks' solution (hereafter called solution A). (Solution A consisted of Ca−Mg free Hanks' solution with phenol red supplemented with 1% Na Citrate · 2 H_2O [Rinaldini, 1959] and 30 mM HEPES [N-2 hydroxyethylpiperazine-N-2-ethanesulphonic acid] buffer, pH 7.3). Hearts were dissected free of the great vessels, and cut into small pieces.

The disaggregation procedure used 0.1% trypsin in solution A and was carried out entirely within a syringe essentially as suggested by Rinaldini (1959).

Cells were plated on agar coated glass slides containing 10 μ wide slits, and incubated at 37° in water saturated air.

Culture Medium

The culture medium initially used was similar to that of Lehmkuhl and Sperelakis (1963), except that fetal or newborn calf serum (GIBCO) was substituted for horse serum. Following the introduction of HEPES buffer, CO_2 was not used at any stage in the culturing procedure.

The standard culture medium was formulated for 500 ml as follows:

Puck's N-15 nutrient medium	200.0 ml
$CaCl_2$, 30 mM stock	1.0
Hanks' solution, 10 X, w/o bicarbonate	22.5
$NaHCO_3$, 1.4% stock	12.5
Fetal (or newborn) calf serum	50.0
HEPES 2 M adjusted to pH 7.3 with 10 N NaOH	7.5
Penicillin and Streptomycin, 5,000 units/ml and 5,000 μg/ml, respectively	1.0
Distilled water	205.5

The medium had the following calculated ionic content in mM: Na^+ 148.0, HCO_3^- 4.6, K^+ 5.8, SO_4^- 0.76, Cl^- 136.7, Mg^{++} 1.16, Ca^{++} 1.54, HPO_4^- 0.162, $H_2PO_3^+$ 1.16, HEPES 30.0. The osmolality was 320 mOsm measured with a Fiske osmometer.

Substrate Preparation

A 2×3 in ×1 mm glass slide was flooded with a 0.5% solution of washed Difco agar kept in a boiling water bath. The slide was then propped up at an angle, agar side down, to drain off the excess and to dry.

In order to make even channels in the agar coating, the slide was placed, agar side up, on the mechanical stage of a microscope and drawn beneath a scalpel blade mounted on a hinged arm. Channels were made about 1 mm apart and measured between 5 and 10 μ in width. In order to convert the slides into culture vessels, epoxy rims (Maraglas) were glued to the slides with General Electric RTV-118 silicone rubber. The dishes were then covered with standard 50 mm glass petri dish covers and sterilized in a drying oven at 120 °C for 30 min. Longer sterilization destroyed the agar's nonadhesive properties.

Optical Apparatus

The culture dishes were observed with a Unitron inverted microscope fitted with a 40× long working distance phase objective. The culture medium was covered with a layer of silicone diffusion pump oil (Dow Corning) to retard evaporation.

Temperature of the culture medium was maintained at 36±1 °C by two thermistor controlled 75 W enlarger bulbs placed below the stage.

In order to allow observations beyond one field diameter without disturbing the preparation, the microscope was mounted on a micrometer-driven slide, independent of the stage.

Recording

A block diagram of the recording arrangement is illustrated in Fig. 1. Voltages were recorded by Bioelectric Instruments NF-1 negative capacity amplifiers connected to the electrodes by chlorided silver wires. For ac studies, the electrode lead-in wires were shielded, the shield on the stimulating electrode being grounded, and that on the recording electrode being driven at unity gain. Each amplifier output was connected to one channel of a Tektronix 3A74 four trace preamplifier in a 561 oscilloscope fitted with a camera.

The output of the recording amplifier was also connected to a Tektronix 2A63 differential amplifier mounted in a 564 storage oscilloscope. The vertical output of the 564 was connected to a Fabritek 1052 signal averager, either directly for pulse experiments, or through a Kron-Hite 330-M tunable bandpass filter for ac experiments. The averager output was

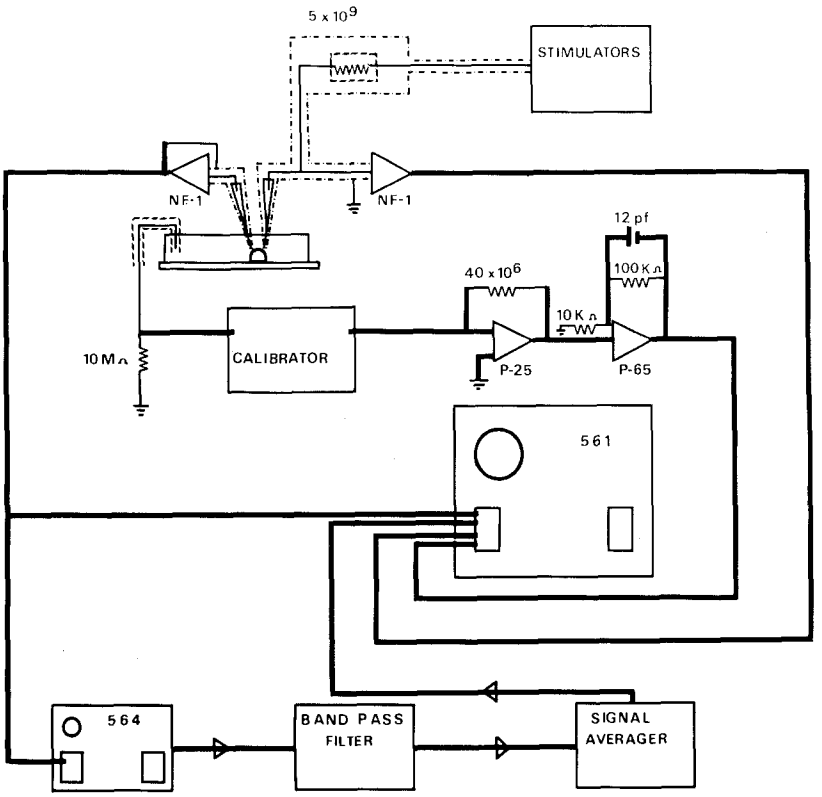

Fig. 1. Diagram showing the electrical recording system. Microelectrode shielding (stimulating electrode shield grounded, recording shield driven at unity gain) was only used for ac measurements. Stimulation was applied through a guarded and shielded 5 Gohm resistor. To average pulse responses, the band pass filter was removed (*see text* for further details)

connected to one channel of the four trace preamplifier enabling averaged records to be photographed.

In order to average ac responses in phase with spontaneous action potentials, a two input "and" gate was used to trigger the averager sweep. One input was connected to the sine wave generator synchronizing output, and the other to the oscilloscope internal trigger, with the result that the averager sweep was triggered by the first ac synch pulse following initiation of the oscilloscope sweep. When the oscilloscope was triggered by an action potential, this method of synchronization allowed a time error of only one oscillation period between the upstroke of an action potential and initiation of the averager sweep.

Stimulus voltages were produced by a Kron-Hite sine wave generator (Model 420-A) in series with two Grass stimulus isolation units driven by two Grass S-4B stimulators. The stimulus voltage was passed through a 5,000 Mohm resistor, guarded and shielded, directly to the input of the stimulating electrode amplifier. In general, no attempt was made to follow the response at the stimulating electrode during stimulation.

The indifferent electrode consisted of a chlorided silver wire connected to the bath directly or through a salt bridge. This was connected to one side of a Bioelectric C-4 calibrator, and to ground with a precision 10 megohm resistor. (This resistor allowed the calibrator to be used for both current and voltage calibration.) The other side of the calibrator

was connected to a current-to-voltage converter with a bandwidth of about 6.8 kHz. The negative capacity of the electrode amplifiers was adjusted to provide the fastest possible rise time without ringing.

Microelectrodes were filled with 3 M KCl and generally had resistances of 40–100 megohm. For ac studies the electrodes were shielded with a thin layer of gold (Hanovia Liquid Gold Division, East Newark, New Jersey).

Experimental Procedure

For quantitative studies, strands of uniform width were chosen. In some cases short cables were obtained by cutting off a short section from a longer strand with a shard of razor blade held in a micromanipulator.

In pulse studies, the stimulating and recording electrodes were inserted, and after recording the electrical response, the recording electrode was moved to a new place in the strand. Records were made only after the penetrations remained stable for a few minutes.

For the ac studies, only two penetrations were required, and these were made at an interelectrode distance of about four to five strand widths. The responses to four different frequencies, usually 100, 200, 400, and 800 Hz were recorded and, if the penetration remained satisfactory, records of the response to other frequencies and to pulses were made. After withdrawal, the shunting capacitance of the stimulating electrode was measured by recording the voltage applied to the stimulating electrode and the total current passed at each of several frequencies. When the series of records was complete, the recording electrode was withdrawn and coupling between the electrodes was checked at a number of frequencies.

Because action potentials caused ac amplifier blocking at high gains, the cells were initially depolarized with 60 mM KCl. After the introduction of the band pass filter, however, spontaneous activity no longer posed a problem since the action potentials contained little power above 100 Hz.

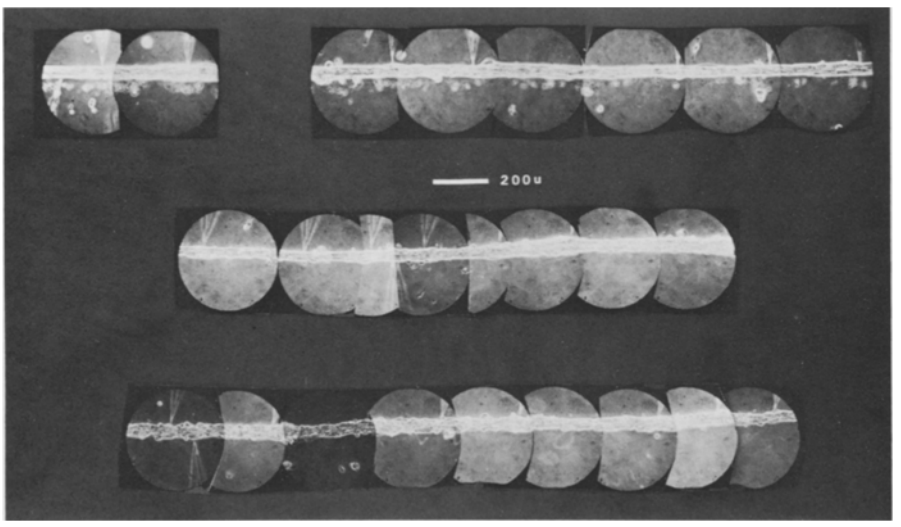

Fig. 2. Photomontage of three strands used in multiple penetration cable studies. The recording electrode appears above the fiber in each frame and the stimulating electrode, which remained stationary, below the fiber. (Although one frame is missing from the upper montage, the distance between adjacent frames was known)

Analysis of Electrical Records

The high frequency ac records were analyzed according to the method of Tasaki and Hagiwara (1957). For strands whose length was considered finite, appropriate approximations to the more complete equations of Falk and Fatt (1964) were made and fit by a least squares computer program.

Several corrections were applied to the ac data prior to analysis. The recording amplifier had a limited bandwidth which reduced the signal amplitude at higher frequencies. This error was corrected by using the following formula:

$$V_{\text{true}} = V_{\text{recorded}}[(f/fo)^2 + 1]^{1/2}$$

where f_0 is the $3db$ bandwidth and f is the frequency in question. [The formula is calculated assuming that the response is that of a simple parallel RC circuit (Aseltine, 1968)]. This correction was never more than 15%.

Another correction was made for the recorded current that passed through the electrode-to-bath capacitance without reaching the cell. I assumed the electrode to be a parallel RC circuit consisting of the tip resistance and the electrode-to-bath capacitance. By measuring the voltage across the stimulating electrode and the current passed as a function of frequency, the capacitance was calculated from a least squares fit to the formula:

$$\left(\frac{I}{V}\right)^2 = C\omega^2 + \frac{1}{R^2} \tag{5}$$

where V and I are, respectively, the peak voltage across and the peak current through the combination, C = capacitance, R = resistance and ω = angular frequency.

With a value for C and the total current, I, the actual current entering the cell, I_c, can be calculated from Eq. 1, realizing that the current passing through the capacitance is $V\omega C$:

$$I_c = (I^2 - (VC\omega)^2)^{1/2}.$$

This correction was significant at the highest frequencies where as much as 50% of the recorded current did not pass through the cells.

Histology

The average width and the length, if considered finite, of the cell strand, and the distance between the electrodes were measured from phase contrast photomicrographs made during the experiment. To determine cross sectional area and membrane area per unit length, the cells were fixed with glutaraldehyde, embedded in Maraglas, and sectioned for light and electronmicroscopy. To emphasize internal membrane systems and cell boundaries, strands were sometimes fixed with lanthanum and permanganate according to Lesseps (1967).

Since an anatomical examination of each strand studied electrically was prohibitively difficult, a statistical approach was adopted which attempted to correlate the cross sectional area and the membrane area per unit length of a strand with the *in vitro* strand width. Strand widths and cross sectional areas were measured on thick section light micrographs, and were correlated by fitting the area to a second order polynomial of the width. (Shrinkage due to glutaraldehyde-osmium fixation and embedding was estimated by fixing, dehydratings and embedding a preparation, under continual observation, on the stage of the microscope. The overall linear shrinkage was estimated to be 17%, which is close to the 20% estimated by Adrian and Peachey (1965). This shrinkage was taken into account in calculating cross sectional areas.)

An average surface to volume ratio was calculated by measuring the cross section of a cell with a planimeter, and its circumference with a map measurer. The circumference was

adjusted for unresolved folding of the membrane by a "folding factor", *FF*, formed by taking the ratio of the exact periphery to an averaged one using high resolution electron micrographs. *FF* averaged 1.45. The fiber cross section times the average surface to volume ratio provided the surface area/unit length. The correlations of morphometric observations were all done by a weighted least squares routine as part of a program that produced as final output a table of *in vivo* strand width and corresponding cross sectional and membrane areas/unit length, with 95% confidence limits.

Results

Initially, quantitative studies were attempted on strands one cell wide, but these strands, together with isolated cells, were difficult to penetrate, exhibited resting potentials of less than −20 mV, and were electrically inexcitable. In fact, the only reliable sign that the electrodes were intracellular was the presence of electrical coupling between two electrodes. Consequently, attention was focused on the multicellular strands. In these strands, the potentials recorded with microelectrodes looked very similar to those reported by others for cultured cells (Sperelakis, 1967; DeHaan & Gottlieb, 1968; Lieberman, 1967). The strands, however, almost always showed the slow transition from "pacemaker potential" (phase 4) into the action potential characteristic of pacemaker cells (Fig. 3). This is in contrast to sheet cultures where latent pacemakers (cells showing an abrupt transition from pacemaker potential to action potential) were much more common. Maximum diastolic potentials were on the order of 50–80 mV and action potentials were on the order of 70–100 mV. The action potentials usually showed no extended plateau, although plateaus were occasionally present (*see* Fig. 4).

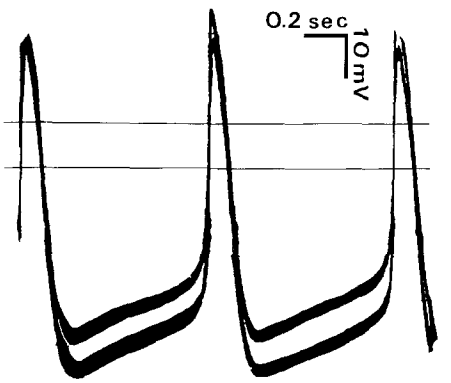

Fig. 3. Typical action potentials observed in cultured strands, recorded with two electrodes 35 μ apart. The voltage baselines for the upper and lower action potentials are indicated approximately by the upper and lower narrow lines respectively. Notice the smooth transition from the pacemaker potential into the action potential characteristic of pacemaker cells

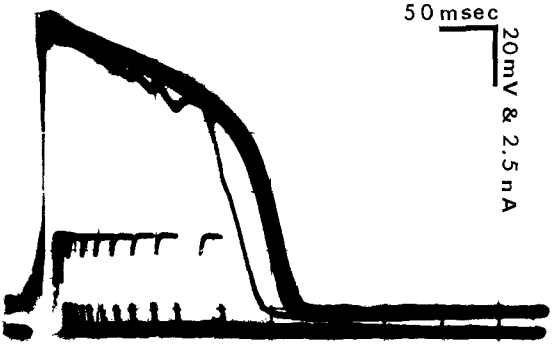

Fig. 4. Multiple exposure showing the effect of constant current hyperpolarizing pulses applied at different times during the plateau in a short (*ca.* 200 μ) fiber. The lower trace is current and the upper is voltage. The action potential was initiated by a strong depolarizing pulse causing the blank space in the current record at the beginning of the sweep. Notice the increase in magnitude of the response to the test pulse with time. The last pulse was sufficiently close to the voltage threshold of phase three, rapid repolarization, to cause early repolarization

One of the most constant features of the cultured strands was the presence of electrical coupling between cells. In two years, during which over a thousand dual penetrations were made, coupling was always found to be present in contiguous tissue.

Effect on Polarizing Current

The effect of current was complicated due to the time-dependent characteristic of the pacemaker potential, and due to anomalous rectification which caused the membrane resistance to decrease with hyperpolarization. The effect of constant current pulses applied to a strand at various times during the pacemaker potential (phase 4) is shown in Fig. 5. In this multiple exposure 0.25 na hyperpolarizing test pulses were applied at different times between the end of repolarization of an action potential (at the left), and threshold (at the right). The response to the test pulse increased as the potential became more positive, suggesting an increase in the membrane slope resistance. Correspondingly, the "on" and "off" time constants increased as phase 4 progressed in time (Fig. 6).

Anomalous rectification was observed when current was applied during phase 4 (*see* Fig. 7). Hyperpolarizing pulses of increasing amplitude were applied, and the slope conductance, i.e., the change in voltage per increment of current, decreased. Fig. 8 shows this effect at different diastolic potentials. With small hyperpolarizing currents, the strand con-

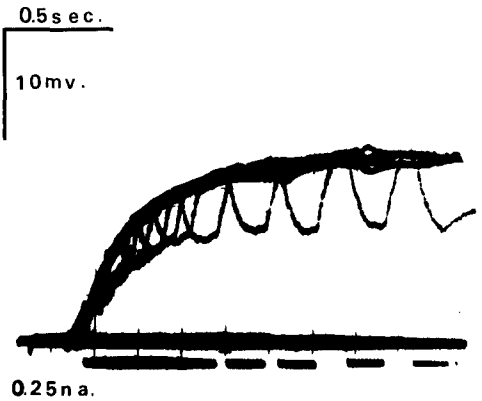

Fig. 5. A multiple exposure showing the effect of 0.25 na, 150 msec, hyperpolarizing pulses applied at different times during the pacemaker potential in a short (70 μ long) fiber. The pacemaker potential proceeds from maximum hyperpolarization at the left to new threshold at the right. (The subthreshold and anode break responses have been photographically removed for clarity)

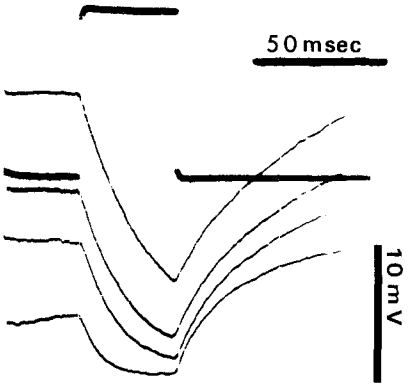

Fig. 6. Multiple exposure showing the effect of 4.3 na hyperpolarizing pulses applied at different phase 4 potentials (negative downward). Stimulating and recording electrodes were 161 μ apart in a long strand. The current record is the dark trace. The sweep was initiated at different potentials and the stimulus was applied 80 msec later. Notice the increase in amplitude and time constant at the more positive potentials

tinued to depolarize with time, but more slowly than without polarization. With stronger currents, the strand hyperpolarized with time (Fig. 9). Notice in Fig. 9 that the slope of the pacemaker potential during the pulse may be seen to go from positive to negative as the transmembrane potential is made negative to the potassium equilibrium potential, approximately -70 mV.

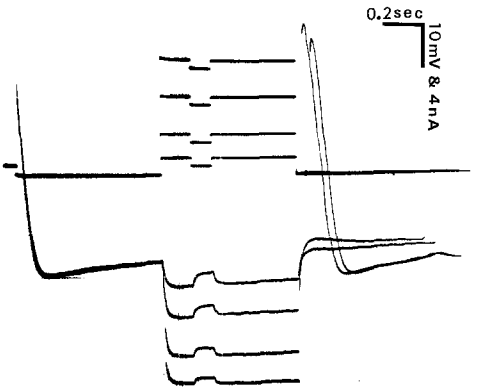

Fig. 7. Multiple exposure illustrating anomalous rectification. During phase 4, the cell was hyperpolarized by varying degrees with constant current pulses, and small constant current depolarizing test pulses were applied. The current records are above and the voltage records below. The response to the test pulse decreased with hyper-polarization (Anode break responses follow release of the stimulus)

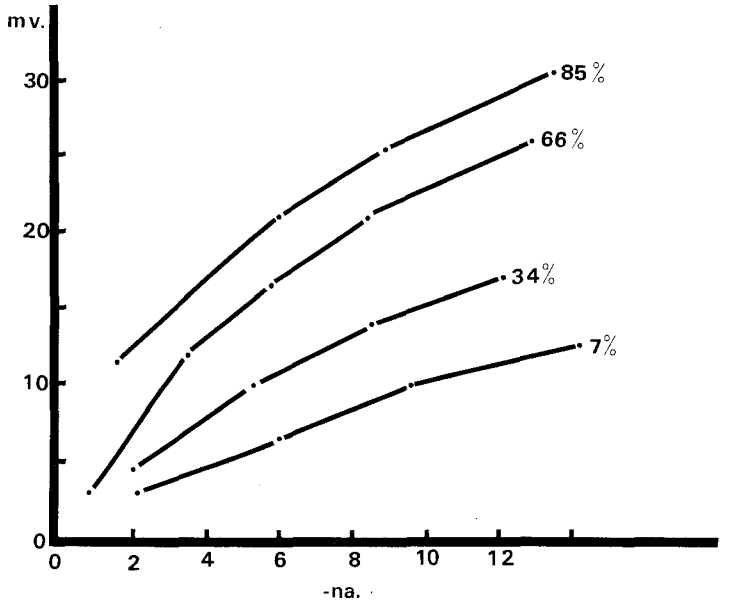

Fig. 8. Typical response of cultured cardiac fibers to hyperpolarizing pulses of different amplitude applied at different times during phase 4. The dots are experimental points, and the lines have been drawn in for clarity. The ordinate represents the voltage response, and the abscissa the applied current. Percentages refer to the membrane potential at which the stimulus was applied, measured as a percentage of the total phase 4 potential variation (i.e., 85 % means a potential 85 % of the way from maximum diastolic potential toward threshold). The increase in transfer resistance during diastole is apparent, and the presence of anomalous rectification is indicated by the curvature of each current-voltage plot. Stimulating and recording electrodes were 26 μ apart in a 60 μ wide strand

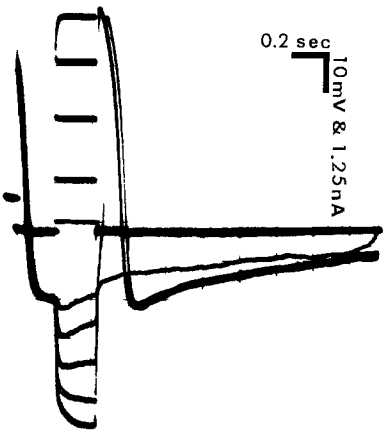

Fig. 9. Multiple exposure of the response of a cultured cardiac fiber to hyperpolarizing pulses of different amplitudes, illustrating reversal of the pacemaker potential. The zero potential level is approximately at the lower end of the voltage-current calibration bar, and the calibration pulse at the beginning of the current trace is 1 na and 50 msec. The end of repolarization of the action potential that triggered the sweep appears at the left of the figure (10 μ wide strand, stimulating and recording electrodes 158 μ apart)

dc Cable Studies

A large number of experiments substantiated the presence of electrical coupling between cells, regardless of the interelectrode distance. Thus, a dc pathway through the strand existed, and were there no macroscopic heterogeneities, one would expect to observe a one-dimensional cable response, i.e. voltage decreasing exponentially with distance. This was tested by choosing the more uniform strands, inserting a polarizing electrode and, with a second electrode, measuring the voltage at different distances. The data from one experiment (the upper strand in Fig. 2), performed without the averager, are presented in Fig. 10. In this experiment, stimulation was applied about 100 msec after the maximum diastolic potential, and the space constant was determined to be 1.3 mm. Several of these experiments were done and the results are shown in Tables 1*a* and 1*b*.

Another type of dc pulse experiment was done using three electrodes, one to polarize and two to record at different distances. The differential voltage between the two recording electrodes and the potential at the nearer one were recorded. These experiments were quite difficult to perform since three simultaneous penetrations had to be maintained, but one experiment was sufficiently stable and the results were included in Tables 1*a* and 1*b*.

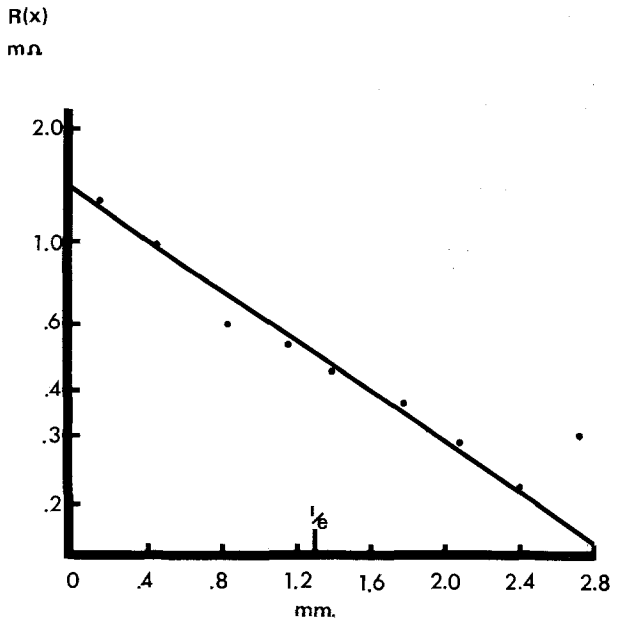

Fig. 10. Results of a multiple penetration, dc cable study. The ordinate represents the transfer resistance, voltage divided by the input current (notice the log scale). The abscissa is the distance from the polarizing electrode. Hyperpolarizing pulses of 12 na were applied 100 msec after the maximum diastolic potential. Dots are experimental points and the line was drawn through the points by eye. The distance at which the transfer resistance falls to 1/e of its maximum value, i.e., the space constant, is indicated

Table 1*a*. Extrinsic electrical properties of tissue cultured cardiac fibers: dc experiments

Expt. No.	Type	Width	R_i	C	R_m (MΩ/cm)			R_0 (MΩ)			λ (mm)			Cond. Vel.
		(μ)	(MΩ/cm)	(μF/cm)	E[a]	M	L	E	M	L	E	M	L	(cm/sec)
1 dc	3 electrode	40	11.9	0.072	0.096	–	0.76	0.64	–	1.28	0.91	–	2.54	–
2 dc	Mult. penet.	40	13.0	0.12	0.34	–	–	1.3	–	–	1.28	–	–	6.8
3 dc	Mult. penet.	26	33.0	–	0.43	–	–	1.85	–	–	1.16	–	–	–
	MEAN	35	19.3	0.096	0.28	–	0.76	1.26	–	1.28	1.1	–	2.54	6.8

[a] E, M and L refer to early, middle and late diastole.

When the capacitative charging could readily be distinguished from the time constant of the pacemaker potential variation, estimates of τ were made from plots of the time to half amplitude *vs.* distance. The slope, equal to $2\lambda/\tau$, was used to solve for τ (Hodgkin & Rushton, 1946).

Table 1*b*. Intrinsic electrical properties of tissue cultured cardiac strands: dc experiments[a]

Expt.	ρ_i	C_m	ρ_m (kΩ/cm²)			τ (msec)			Width	Cross sect. area	Surface area/1
	(Ω/cm)	(μF/cm²)	E	M	L	E	M	L	(μ)	(μ²)	(μ²/cm)
1 dc	110	0.93	7	–	59	–	55	–	40	923	774
2 dc	120	1.55	26	–	–	41	–	–	40	923	774
3 dc	146	–	17	–	–	–	–	–	26	442	407
MEAN	125	1.24	17	–	59	41	55	–	35	762	651

[a] Abbreviations as in Table 1*a*; cross sectional area estimates based on total cross section, including vacuoles.

ac Cable Studies

For angular frequencies whose periods were short compared to the membrane time constant, the membrane equivalent circuit may be approximated by its capacitance alone. (An example of the insensitivity of the impedance at high frequencies to the membrane changes taking place during the pacemaker potential is shown in Fig. 11.) The ac data were fitted to a straight line graph according to the method of Tasaki and Hagiwara (1957), after corrections for bandwidth and stray capacity were made as described in *Materials and Methods*. The results of one ac study are shown in Fig. 12. Using the values of core resistivity and membrane capacity from these curve fits, the response of the strand to low frequency, or pulse polarization, was used to derive the membrane resistance. Results of the ac experiments are presented in Tables 2*a* and 2*b*.

In three cases in which sufficient data was available the membrane capacity was measured using the "foot" of the action potential as described by Tasaki and Hagiwara (1957):

$$C = 1/(R_i\, T_{AP}\, v^2).$$

Using v of spontaneous action potentials (assumed constant), the average capacity calculated in this way was 82 nF/cm compared to 78 nF/cm using injected currents (ac and dc).

In a few cases in which pronounced plateaus were present, test pulses were applied during the plateau in order to examine the resistance changes and to determine whether or not repolarization was voltage sensitive. The results of a typical experiment are shown in Fig. 4. In this multiple exposure, 4 na, 15 msec, hyperpolarizing test pulses were applied during the plateau. The later the pulse was applied, the larger was the voltage response until the last (right most pulse) produced an early repolarization.

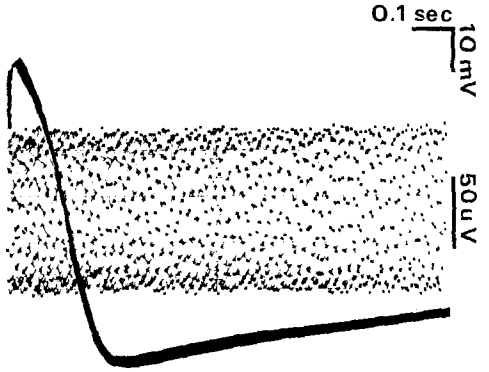

Fig. 11. The high frequency impedance of the strand is independent of changes taking place during the pacemaker potential. The upper voltage calibration refers to the action potential, and the lower to the averaged ac response. Polarization (100 Hz, 1 na) synchronized with the action potential was applied intracellularly, and the response was recorded 35 μ away using a signal averager. Due to the rapid oscillation of the polarization on this time scale, individual cycles cannot be resolved, but it is clear from the envelope of the response that there is little change in amplitude from plateau to threshold

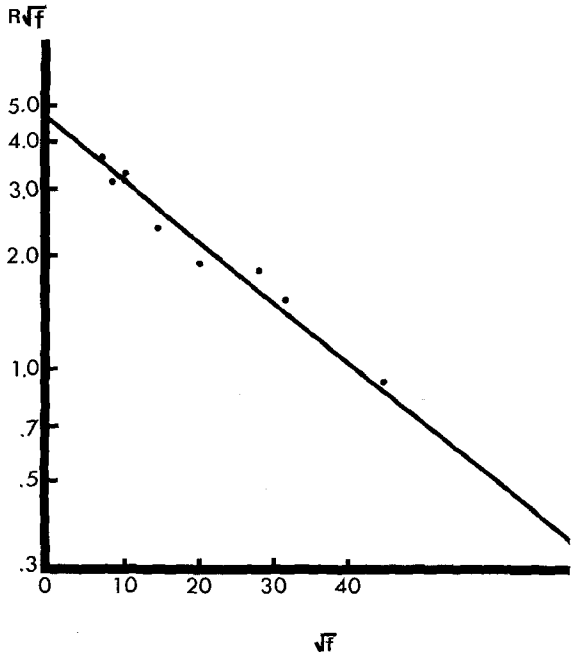

Fig. 12. A Tasaki and Hagiwara (1957) type of plot showing current (I) injected at $x=0$, and the amplitude of the voltage response (v) at $x=265$ μ as a function of frequency (f). $R=V/I$ has the units of MΩ and f is in Hz. Data are plotted as $\ln R\sqrt{f}$ versus $\sqrt{f}$. The intercept and slope yield values for the core resistance and membrane capacity

Table 2*a*. Extrinsic electrical properties of tissue cultured cardiac strands: ac experiments

Expt. No.	Length	Width	R_i		R_m (MΩ/cm)			R_0 (MΩ)			λ (mm)			Cond. Vel.
	(μ)	(μ)	(MΩ/cm)	(μF/cm)	E[a]	M	L	E	M	L	E	M	L	(cm/sec)
1 ac[b]	inf.	35	12.0	0.030	(0.39 NB)			(0.48 NB)			(1.8 NB)			
2 ac	250	50	12.0	0.075	(0.18 NB)			(0.23 NB)			(0.39 NB)			
3 ac	inf.	35	34.7	0.052	0.46	–	–	1.99	–	–	1.15	–	–	
4 ac	980	42	30.1	0.163	0.51	1.37	–	–	1.95	3.16	–	1.3	2.1	
5 ac	inf.	37	102.0	0.128	–	–	–	–	–	–	–	–	–	
6 ac	inf.	30	22.1	0.125	0.69	0.94	2.9	1.95	2.3	4.0	1.7	2.1	3.6	
7 ac	inf.	37	12.1	0.122	–	1.38	–	–	2.0	–	–	3.3	–	
8 ac	inf.	50	23.5	0.115	0.04	0.14	–	0.52	1.1	–	0.44	0.83	–	
9 ac	inf.	40	26.2	0.119	–	–	–	–	–	–	–	–	–	
10 ac	inf.	30	14.1	0.093	0.27	0.45	1.5	0.91	1.27	2.25	1.3	1.8	3.2	31
11 ac	inf.	32	47.6	0.075	–	–	–	–	–	–	–	–	–	
12 ac	inf.	30	28.4	0.087	0.14	1.6	4.2	1.98	3.2	5.9	0.6	2.3	3.8	13
MEAN		37	30.4	0.099	0.32	0.83	2.49	1.11	1.97	3.8	0.95	1.9	3.2	22

[a] E, M and L refer to early, middle and late diastole respectively; NB means not beating spontaneously.
[b] KCl depolarized.

Table 2*b*. Intrinsic electrical properties of tissue cultured cardiac strands: ac experiments[a]

Expt. No.	ρ_i	C_m	ρ_m (KΩ/cm²)			τ (msec)			Width	Cross sect. area	Surface area/l
	(Ω/cm)	(μF/cm²)	E	M	L	E	M	L	(μ)	(μ²)	(μ²/cm)
1 ac[b]	87	0.47	(25 NB)			(12 NB)			35	731	632
2 ac	164	0.68	(20 NB)			(14 NB)			50	1,370	1,097
3 ac	253	0.82	29	–	–	24	–	–	35	731	632
4 ac	303	1.94	–	43	115	–	83	220	42	1,006	836
5 ac	822	1.81	–	–	–	–	–	–	37	806	687
6 ac	124	1.98	35	47	145	80	115	260	30	563	502
7 ac	98	1.77	–	95	–	–	168	–	37	806	687
8 ac	322	1.05	4	15	–	5	18	–	50	1,370	1,097
9 ac	242	1.54	–	–	–	–	–	–	40	923	774
10 ac	79	1.85	14	23	75	25	42	137	30	563	502
11 ac	299	1.36	–	–	–	–	–	–	32	628	553
12 ac	143	1.73	7	80	211	12	136	360	30	563	502
MEAN	245	1.46	16	50	136	29	94	269	37	838	708

[a] Abbreviations as in Table 2*a*; Area estimates based on total cross section, including vacuoles.
[b] KCl depolarized.

It is evident that the resistance increases during phase two, and that repolarization is indeed voltage sensitive. This is in accord with work on other cardiac tissue (Weidmann, 1951; Cranefield & Hoffman, 1958; Fozzard & Sleator, 1967).

Histology

Light microscopy of *in vitro* strands was not particularly revealing due to the thickness of the strands. However, large vacuoles were sometimes visible on the strand periphery and occasionally cell outlines were apparent (Fig. 2). The transverse sections of embedded tissue revealed that they were "D" shaped, flat side against the glass, and otherwise quite variable in shape. The only subcellular detailed resolved in the light microscopic sections were numerous unstained areas, hereafter called *vacuoles.*

The strands were comprised of a number of cells of irregular cross section. The cytoplasm appeared disorganized as compared to adult atrial or ventricular cardiac tissue (*cf.* McNutt & Fawcett, 1969; Hama & Kanaseki, 1967; Johnson & Sommer, 1967), but not grossly dissimilar from embryonic ventricular tissue (Challice, 1966). Numerous vacuoles were present, some of which were not bounded by membranes. These unbounded vacuoles may be the same structures noted by Gross and Riedel (1969) in association with sites of pulsatile activity in chick heart cells in planar cultures. In measuring the strand cross sectional areas, two tabulations were made, area including vacuoles, and area minus vacuoles. Vacuoles accounted for about 10% of the total cross section. Results of the area calculations are included in Tables 1*b* and 2*b*. The 95% confidence limits on the cross sectional area were about 15% of the mean.

Myofibrils were seen in almost every cell in every section so that in some sense the preparation was homogeneous. Myofibrils tended to be found near the sarcolemma and to run parallel to the cell axis but were sometimes seen in other orientations. Polyribosomes were seen in abundance, often in the helical array reported by Cedergren and Harary (1964).

Lanthanum, which, as Revel and Karnovsky (1967) showed, stains the transverse system in mouse heart, did not stain any of the internal membranes of cells in the strands. Since these cells apparently did not possess a transverse tubular system, the membrane area per unit length was estimated by simply following the boundary of each cell with a map measurer. The results of the calculations on the average membrane area per unit length are included in Tables 1*b* and 2*b*. The 95% confidence limits on surface area were about 40% of the mean. The myoblast morphometry results are close to those reported by Lieberman *et al.* (1975). The average surface to volume ratio was 0.87/μ compared to the 0.88/μ reported by Lieberman *et al.* This corresponds to an equivalent cell diameter of 4.5 μ.

High resolution micrographs showed areas of close apposition between cells which permitted lanthanum penetration, suggesting contact via gap junctions.

Discussion

The results of the present investigation support very strongly the existence of electrical coupling between cardiac cells in tissue culture. The fact that in the strands voltage decayed exponentially with distance for more than 10 cell lengths means that electrical coupling between cells must exist, and in fact, must be very efficient, given the long space constants relative to the size of the constituent cells.

Cable Parameters

Use of the cable equations to determine passive properties assumes that the resistances are linear. The extent to which the observed nonlinearities affect determination of the linear cable properties is difficult to estimate analytically. However, several qualitative arguments support the fact that the linear model is still a reasonable approximation.

In the present experiments nonlinearity of the membrane resistance (anomalous rectification) would have caused the graph of log voltage *vs.* distance to show a concavity for data obtained with hyperpolarizing test pulses. As is clear from Fig. 10 such an effect, if present, was masked by point scatter due to random errors. Since the experiment illustrated in Fig. 10 was performed with relatively high polarizing currents, it is apparent that anomalous rectification did not seriously interfere with the determination of the cable parameters.

Since the cells were spontaneously active, efforts were directed at determining instantaneous values of the cable parameters. Two factors were considered in assessing the accuracy of these measurements: homogeneity of the cable properties and errors caused by the finite time required to make measurements. The first factor concerns the question of whether the cell properties change equally over the whole strand, or whether there is a gradient, for example, from pacemaker to nonpacemaker cells. In general, phase 4 depolarization occurred virtually simultaneously in all cells of a strand, the voltage being approximately equal in cells hundreds of micra apart. This suggests that the instantaneous cable properties did not vary with distance along the strand (except as perturbed by the stimulating current) during most of phase 4.

Table 3. The error in the computed value of membrane time constant caused by a ±10% error in the voltage characterizing the end of capacitive charging; as a function of distance between the polarizing and recording electrodes, and the voltage reference point

Reference point as a percentage of final value	Interelectrode distance measured in space constants	Error in time constant in %
84 %	0.0	−43, +37
	0.5	−30, +31
	1.0	−24, +28
50 %	0.0	−27, +28
	0.5	−16, +13
	1.0	−11, +10

The second factor, concerned with errors caused by finite measurement times, arose because of the gradual change in membrane resistance during phase 4. The magnitude of the potential change produced by a polarizing test pulse was best estimated by applying the pulse at different times during phase 4, and measuring the instantaneous displacement from the envelope of the response (*cf.* Fig. 6). The rise and fall times of the response, however, were subject to large errors since the shape of the charging curve was distorted by phase 4 resistance changes. The end of capacitative charging was particularly difficult to estimate. The error in the calculated time constant caused by a small (10 %) error in estimating the end of capacitive charging was calculated by a computer solution for the pulse response of a cable. The results are shown in Table 3.

The dc cable studies proved to be difficult to perform, primarily because of the inability to consistently obtain a number of successive penetrations without dislodging the polarizing electrode or damaging the fiber. In addition, the requirement for synchronization of the test pulse with the action potential limited the averager repetition rate, and required a that penetration be maintained for long periods of time. For these and other technical difficulties, the ac method of determining cable properties was preferred.

ac Cable Parameter Studies

Inherent in this analysis is the assumption that the strand can be considered a simple parallel RC cable. Falk and Fatt (1964) pointed out that the ac method of analysis, using only amplitude responses and ignoring phase relationships, is insensitive to deviations from the simple cable model. Thus, Tasaki and Hagiwara (1957), using amplitude information

alone, were unable to find more than one time constant in their analysis of the frog sartorius muscle cell, whereas Falk and Fatt, using both amplitude and phase information, showed the presence of at least two time constants. However, a full impedance study using phase and amplitude information was not undertaken in the present work for several reasons. Firstly, with high resistance electrodes, the recording bandwidth was limited, and phase distortion began at low frequencies. Secondly, the strands were not of consistently even diameter, precluding precise analysis. Since the histology showed that there was no tranverse tubular system, and the cells were not sufficiently close packed to produce a significant series resistance between the inside and outside of the strand, the simple RC cable model is probably correct to first order.

The results of the ac experiments are more precise than the pulse experiments for a number of reasons. Only two penetrations were required. Secondly, the bandwidth of the recording system was restricted by a bandpass filter, increasing the signal-to-noise ratio, and permitting the use of low polarizing currents. (In general, the voltage at the stimulating electrode was less than 350 μV.) Thirdly, at high frequencies the membrane admittance was completely dominated by the membrane capacitance, so that nonlinearities of the membrane resistance were of no consequence. And finally, since the high frequency polarization permitted a rapid sweep rate of the averager, an experiment could be completed in minutes as opposed to hours for the multiple penetration experiments. The high frequency measurements, although placing demands upon the electrical system accuracy, avoided the need to numerically fit the data to a cable equation with time dependent properties as Lieberman *et al.* (1975) were forced to do in order to extract usable parameters.

The determination of the membrane resistance with pulses, or low frequency polarization, is subject to the same kinds of nonlinearity problems as the multiple penetration cable experiments. However, only one parameter, the membrane resistance, must be determined from these more variable data.

For reference, the reported values of intrinsic membrane properties for a number of tissues are presented in Table 4.

Core Resistivity and Intercellular Junctions

The mean core resistivity measured in the ac experiments was 245 ohm/cm when referred to the entire cross section of the fiber. If space occupied by vacuoles is deducted, the value drops to about 227 ohm/cm. These

Table 4. Passive electrical properties reported for various tissues[a]

Ref.	Type of Tissue	ρ_m ($k\Omega \cdot cm^2$)	ρ_i ($\Omega \cdot cm$)	C_m ($\mu F/cm^2$)
	Cardiac Muscle			
1.	Frog ventricle strips	2.6	460	1.2
2.	Purkinje fibers (ungulate)	19.	105	1.2
3.	Trabeculae (ungulate)	9.1	470	0.8
4.	Tunicate heart	0.23	2,800	1.6
5.	Cultured chick (strands)	20.5	180	1.54
6.	Cultured chick (strands)[b]	16–136	245	1.46
7.	Cultured chick sheet	14	418	–
	Smooth Muscle			
8.	Guinea pig taenia coli	25.	125[c]	3.
	Skeletal Muscle			
9.	Frog sartorius (without T-syst.)	3.8	192	2.2
10.	Frog slow fiber	29.	250[c]	2.5
	Nerve			
11.	Lobster	2.3	60	1.3
12.	Squid	0.7	30	1.
13.	Crab	5.	40	1.1

[a] References for measurements quoted in the table are: Van der Kloot & Dane (1964); Mobley & Page (1972); Trautwein *et al.* (1956); Kriebel (1967, 1968); Lieberman *et al.* (1975); This paper; Hyde *et al.* (1969); Tomita (1966); Gage & Eisenberg (1969); Adrian & Peachey (1965); Hodgkin & Rushton (1946); Curtis & Cole (1938); Cole & Hodgkin (1939); and Hodgkin (1947).

[b] dual values refer to early and late phase 4, respectively.

[c] assumed.

values are about two times higher than Weidmann (1952) and Fozzard (1966) reported for Purkinje fibers, but they are in the range reported by Schwan (1965) for high frequency measurements in heart, and are close to the values reported for skeletal muscle (see Table 4).

Although no systematic anatomical study was made of the area of nexal junctions, I would say that 10% is an upper limit for the percentage of total membrane area devoted to gap junctions. (Mobley & Page, 1972, estimate 15% for the ungulate Purkinje fiber.) If so, then for an average fiber with a longitudinal resistance of 30 Mohms/cm and a surface area of about 700 μ^2/cm, the maximum possible junctional resistance, is approximately 20 ohm/cm^2, assuming all current flows through the junctions and cytoplasmic resistance is negligable compared to the junctional resistance. Weidmann (1966) estimated 3 ohm/cm^2 for the junctional mem-

brane. The junctional resistance does not appear to change significantly during action potential phases 2, 4 and probably 3. Thus the resistance between cells is sufficiently low to serve as the means of impulse propagation via local current spread, and probably is not a mechanism for dynamically altering the properties of cardiac tissue during activity.

Membrane Capacity

The average membrane capacity determined in the present experiments is 1.46 $\mu F/cm^2$. This is comparable to that reported for nerve, red cells and various other cells lacking a transverse tubular system. The recent work of Mobley and Page (1972) on Purkinje fibers indicates a capacity of about 1 $\mu F/cm^2$ (*see* Table 4).

Membrane Resistance

I have implicitly assumed that the membrane resistance during phase 4 is primarily time- and not voltage-dependent. There remains the possibility that the apparent resistance changes are really manifestations of a rapidly relaxing voltage-dependent conductance which has a negative resistance region in the potential range covered by the pacemaker potential (Smith, Barker & Gainer, 1975). However, in the absence of conflicting data, I shall assume the simpler model in which the resistance changes are not strongly voltage dependent, i.e., linear. (*See also* Lieberman *et al.*, 1975.)

The most interesting property of the membrane resistance determined in the present study is the variation during the pacemaker potential, from 16 kohm $\cdot$ cm^2 just following repolarization, to 130 kohm $\cdot$ cm^2 near threshold, a change by a factor of about 8. In their cultured strand preparation, Lieberman *et al.* measured a two-fold change in R_m over approximately 20% of the diastolic interval (Lieberman *et al.*, 1975; Fig. 7*B*). A probably unwarranted but suggestive extrapolation of the data to full diastole would suggest a change in R_m of about a factor of 10. The figure for early phase 4, 16 kohm/cm^2, is comparable to the 20 kohm/cm^2 reported by Mobley and Page (1972) for Purkinje fibers at about the same time in diastole.

If these membrane properties apply to single cells in culture, the input resistances would be on the order of $10^9 - 10^{10}$ ohms. The extremely high input resistance of these single cells has undoubtedly accounted for the

difficulty in obtaining successful penetrations (De Haan & Gottlieb, 1968; Lehmkuhl & Sperelakis, 1963; Lieberman *et al.*, 1975).

Comparing the results of this study with those of Lieberman *et al.* (1975) on a tissue cultured strand preparation, all the intrinsic membrane cable parameters were extremely close to those reported here for early diastole (*see* Table 4). Lieberman *et al.*'s strand interestingly did not show the anomalous rectification found here. Their preparation had a different morphology consisting of myoblasts surrounded by a coating of fibroblasts (Purdy, Lieberman, Roggeveen & Kirk, 1972). The different strand structures may be attributed to different culture conditions, in particular the lack of embryo extract and low bicarbonate levels in my media, both of which tend to inhibit fibroblast growth. Lieberman's group also used older hearts which show less automaticity.

Teleologically, the changes in membrane resistance observed during the pacemaker potential may have importance in the suppression of ectopic activity in normally spontaneous pacemaking regions of the heart.

A simplistic analysis of the safety factor (SF) for propagation calculated from Rushton's (1937) formula $SF = v\,\tau/\lambda$, would suggest that the safety factor for propagation in my preparation increases by a factor of 3 during the pacemaker potential (assuming constant v). An increase in conduction velocity would tend to exaggerate the increase in SF.

In fact, such increases in the safety factor were observed (although not quantitated) in the pulse experiments. Depolarizing test pulses were not normally used since they tended to cause action potentials in later diastole which interfered with the measurements. In spontaneously active cell masses another factor exists which may play a role in increasing the safety factor during diastole. As diastole progresses, the space constant increases and may become comparable to a characteristic dimension of the tissue, reducing the dimensionality of current spread. This would tend to make the tissue more isopotential and synchronous.

This research was supported by P.H.S. Grant No. 2 TI GM 1006.

References

Adrian, R.H., Peachey, L.D. 1965. The membrane capacity of frog twitch and slow muscle fibers. *J. Physiol. (London)* **181**:324

Aseltine, J.A. 1958. Transform Methods in Linear Systems Analysis. McGraw Hill, New York

Cedergren, B., Harary, I. 1964. *In vitro* studies on single beating rat heart cells: VI. Electron microscopic sudies of single cells. *J. Ultrastruct. Res.* **11**:428

Challice, C.E. 1966. Studies on the microstructure of the heart. *J. R. Microsc. Soc.* **85**:1

Cole, K.S., Hodgkin, A.L. 1939. Membrane and protoplasm resistance in the squid giant axon. *J. Gen. Physiol.* **22**:671

Cranefield, P.F., Hoffman, B.F. 1958. Propagated repolarization in heart muscle. *J. Gen. Physiol.* **41**:633

Curtis, H.J., Cole, K.S. 1938. Transverse electric impedance of squid giant axon. *J. Gen. Physiol.* **21**:757

DeHaan, R.L., Fozzard, H.L. 1975. Membrane response to current pulses in spheroidal aggregates of embryonic heart cells. *J. Gen. Physiol.* **65**(2):207

DeHaan, R.L., Gottlieb, S.H. 1968. The electrical activity of embryonic chick heart cells isolated in tissue culture singly or in interconnected cell sheets. *J. Gen. Physiol.* **52**:643

Falk, G., Fatt, D.P. 1964. Linear electrical properties of striated muscle fibers observed with intracellular electrodes. *Proc. R. Soc. London B.* **160**:69

Fozzard, H.A. 1966. Membrane capacity of the cardiac Purkinje fiber. *J. Physiol.* (*London*) **182**:255

Fozzard, H.A., Sleator, W. 1967. Membrane ionic conductance during rest and activity in guinea pig atrial muscle. *Am. J. Physiol.* **212**:945

Gage, P.W., Eisenberg, R.S. 1969. Capacitance of the surface and transverse tubular membrane of frog sartorius muscle fibers. *J. Gen. Physiol.* **53**:267

Giebisch, G., Weidmann, S. 1967. Membrane currents in mammalian ventricular heart muscle fibers using a "voltage-clamp" technique. *Helv. Physiol. Pharmacol. Acta* **25**:189

Gross, W.O., Riedel, B. 1969. Asphalt-colored spots of isolated functional heart muscle cells in culture. *Exp. Cell Res.* **54**:237

Hama, K., Kanaseki, T. 1967. A comparative microanatomy of the ventricular myocardium. *In:* Electrophysiology and Ultrastructure of the heart. T. Sano, V.Mizohira and K. Matsuda, editors. pp. 27–40. Bunkodo Co., Tokyo, Japan

Hodgkin, A.L. 1947. The membrane resitance of a non-medullated nerve fiber. *J. Physiol.* (*London*) **106**:305

Hodgkin, A.L., Rushton, W.A.H. 1946. The electrical constants of a crustacean nerve fiber. *Proc. R. Soc.* (*London*) *S. B.* **133**:444

Hyde, A., Blondel, B., Matter, A., Cheneval, J.P., Filloux, B., Girardier, L. 1969. Homo and heterocellular junctions in cell cultures: An electrophysiological and morphological study. *In:* Progress in Brain Research. K. Akert and P.G.Waser, editors. Vol. 31. pp. 238–281. Elsevier, Amsterdam

Johnson, E.A., Sommer, J.R. 1967. A strand of cardiac muscle. Its ultrastructure and the electrophysiological implications of its geometry. *J. Cell Biol.* **33**:103

Johnson, E.A., Tille, J. 1960. Changes in polarization resistance during the repolarization phase of the rabbit ventricular action potential. *Aust. J. Exp. Biol. Med. Sci.* **38**:509

Jongsma, H.J., van Rijn, H.E. 1972. Electrotonic spread of current in monolayer cultures of neonatal rat heart cells. *J. Membrane Biol.* **9**:341

Kriebel, M.E. 1967. Conduction velocity and intracellular action potentials of the tunicate heart. *J. Gen. Physiol.* **50**:2097

Kreibel, M.E. 1968. Electrical characteristics of tunicate heart cell membranes and nexuses. *J. Gen. Physiol.* **52**:46

Lehmkuhl, D., Sperelakis, N. 1963. Transmembrane potentials of trypsin-dispersed chick heart cells. *Am. J. Physiol.* **205**:1213

Lesseps, R.J. 1967. Removal by phospholipase C of a layer of lanthanum staining material to the cell membrane in embryonic chick cells. *J. Cell Biol.* **34**:173

Lieberman, M. 1967. Effects of cell density and low K on action potentials of cultured chick heart cells. *Circ. Res.* **21**:879

Lieberman, M. 1973. Electrophysiological studies on a synthetic strand of cardiac muscle. *Physiologist* **16**:551

Lieberman, M., Sawanobori, T., Kootsey, J.H., Johnson, E.A. 1975. A synthetic strand of cardiac muscle. Its passive electrical properties. *J. Gen. Physiol.* **65**(4):527

McNutt, N.S., Fawcett, D.W. 1969. Ultrastructure of the cat myocardium, atrial muscle. *J. Cell Biol.* **42**:46

Mobley, B.A., Page, E. 1972. The surface area of sheep Purkinje fibers. *J. Physiol. (London)* **220**:547

Purdy, J.E., Lieberman, M., Roggeveen, A.E., Kirk, R.G. 1972. Synthetic strands of cardiac muscle. *J. Cell Biol.* **55**:563

Revel, J.P., Karnovsky, M.J. 1967. Hexagonal array of subunits in intercellular junctions of the mouse heart and liver. *J. Cell Biol.* **33**:C7

Rinaldini, L.M. 1959. An improved method for isolation and quantitative cultivation of embryonic cells. *Exp. Cell Res.* **16**:477

Rougier, O., Vassort, G., Stampfli, R. 1968. Voltage clamp experiments on frog atrial heart muscle fibers with the sucrose gap technique. *Pfluegers Arch. Gesamte Physiol. Menschen Tiere* **301**:91

Rushton, W.A.H. 1937. Initiation of the propagated disturbance. *Proc. R. Soc. London B* **124**:210

Sachs, F. 1969. Electrophysiological properties of tissue cultures heart cells grown in a linear array. Thesis. Upstate Medical Center. Syracuse, N.Y.

Schwan, H.P. 1965. Electrical equivalent circuit of heart muscle. (Discussion) J.W. Woodbury and A.M. Gordon. *J. Cell. Comp. Physiol.* **66** (*Suppl. 2*):35

Smith, T.G., Barker, J.L., Gainer, H. 1975. Requirements for bursting pacemaker potential activity in molluscan neurons. *Nature (London)* **253**:450

Sperelakis, N. 1967. Electrophysiology of cultured heart cells. *In:* Electrophysiology and Ultrastructure of the Heart. T. Sano, V. Mizuhira and K. Matsuda, editors. pp. 81–108. Bunkodo Co., Tokyo

Tasaki, I., Hagiwara, S. 1957. Capacity of muscle fiber membrane. *Am. J. Physiol.* **188**:423

Tomita, T. 1966. Membrane capacity and resistance of mammalian smooth muscle. *J. Theor. Biol.* **12**:216

Trautwein, W., Kuffler, S.W., Edwards, C. 1956. Changes in membrane characteristics of heart muscle during inhibition. *J. Gen. Physiol.* **40**:135

Valdiosera, R., Clausen, C., Eisenberg, R.S. 1964. Impedance of frog skeletal muscle fibers in various solutions. *J. Gen. Physiol.* **63**:460

Van der Kloot, W.G., Dane, B. 1964. Conduction of the action potential in the frog ventricle. *Science* **146**:74

Weidmann, S. 1951. Effect of current flow on the membrane potential of cardiac muscle. *Am. J. Physiol.* **115**:227

Weidmann, S. 1952. The electrical constants of Purkinje fibers. *Am. J. Physiol.* **118**:348

Weidmann, S. 1955. Effects of calcium ions and local anesthetics on electrical properties of Purkinje fibers. *Am. J. Physiol.* **219**:568

Weidmann, S. 1966. The diffusion of radipotassium across intercalated disks of mammalian cardiac muscle. *J. Physiol. (London)* **187**:323